Applied Radiation and Isotopes 174 (2021) 109776

Contents lists available at ScienceDirect

Applied Radiation and Isotopes

journal homepage: www.elsevier.com/locate/apradiso

# Impact of radiobiological models on the calculation of the therapeutic parameters of Grid therapy for breast cancer

Farshid Mahmoudi [a], Nahid Chegeni [a,*], Ali Bagheri [b], Jafar Fatahi Asl [c], Mohammad Taghi Batiar [d]

[a] Department of Medical Physics, Faculty of Medicine, Ahvaz Jundishapur University of Medical Sciences, Ahvaz, Iran
[b] Interventional Radiotherapy Ward, Department of Radiation Oncology, Jundishapur University of Medical Sciences, Ahvaz, Iran
[c] Department of Radiology Technology, School of Allied Medical Sciences, Jundishapur University of Medical Sciences, Ahvaz, Iran
[d] Department of Nuclear Engineering, Faculty of Nuclear Sciences, Shahid Beheshti University, Tehran, Iran

ARTICLE INFO

*Keywords:*
Grid therapy
Therapeutic ratio
Bystander effect
Radiobiological model
Breast cancer

ABSTRACT

Therapeutic advantages of Grid therapy have been demonstrated in several theoretical studies using the standard linear-quadratic (LQ) model. However, the suitability of the LQ model when describing cell killing at highly modulated radiation fields has been questioned. In this study, we have applied an extended LQ model to recalculate therapeutic parameters of Grid therapy. This study shows that incorporating the bystander effects in the radiobiological models would significantly change the theoretical predictions and conclusion of Grid therapy, especially at high dose gradient fields.

## 1. Introduction

Several factors make the treatment of advanced bulky tumors difficult. Poor blood flow in the hypoxic region of large tumors makes them resistant to radiation, and deep-seated tumors limit depth dose distribution. Furthermore, a large volume of the normal tissue involved in the treatment area of bulky tumors, along with the large doses required to suppress such tumors, cause high toxicity to the skin and decrease normal tissue tolerance (Penagaricano et al., 2009; Asur et al., 2015; Huhn et al., 2006; Dubben et al., 1998).

Various treatment modalities such as hyper fractionation, accelerated fractionation, intensity-modulated radiotherapy (IMRT), and volumetric modulated arc therapy (VMAT) have been introduced to overcome such limitations. However, the local control of bulky malignant tumors remains a challenge for oncologists due to limited normal tissue tolerance (McMahon et al., 2015; Meigooni et al., 2005; Mohiuddin et al., 1999).

Grid therapy is an adaptation of a concept in radiation therapy, which is utilized to treat tumors that do not respond to conventional radiotherapy. In this technique, an external block is used to shield an open X-ray field partially and convert it to a set of pencil beam radiation fields. A high dose of radiation (usually, 15–20 Gy) in a single fraction is delivered to the target volume in a non-uniform pattern so that only the volume under the open areas of the Grid receives primary radiation; the rest receives only scattered radiation (Mohiuddin et al., 1996, 1999).

Therapeutic advantages of Grid therapy have been demonstrated by both theoretical modelling (Gholami et al., 2016; Zwicker et al., 2004) and clinical studies (Huhn et al., 2006; Mohiuddin et al., 1999; Choi et al., 2019; Kaiser et al., 2013). Presently, the theoretical calculations are usually based on the linear-quadratic (LQ) model for the calculation of the therapeutic ratio (TR) and geometric sparing factor (GSF) (Gholami et al., 2016, 2017; Zwicker et al., 2004). Theoretical analyses based on the LQ model show that the Grid efficiency may be affected by various factors, such as the geometrical design of Grid blocks, type of tumor, delivered dose, and normal tissue' radiosensitivity (Gholami et al., 2016, 2017; Zwicker et al., 2004; Zhang et al., 2014). However, in recent years, the suitability of the LQ model for predicting cell survival fraction (SF) in highly modulated radiation fields has become the subject of debate. The standard LQ model's parameters are obtained in the uniform radiation field and do not incorporate the bystander effect, which seems to play an important role in the modulated field. Furthermore, some experimental studies have shown that the survival in non-uniform radiation fields differs significantly from that of predicted by the conventional LQ model (Asur et al., 2015; Suchowerska et al., 2005; Bromley et al., 2008; Peng et al., 2017; Butterworth et al., 2011). Recently, Peng et al. (2017) have developed a predictive model with

* Corresponding Author. Department of Medical Physics, Jundishapur University of Medical Sciences, Ahvaz, Iran.
*E-mail addresses:* farshidmahmoudi71@yahoo.com (F. Mahmoudi), chegenin@gmail.com (N. Chegeni).

https://doi.org/10.1016/j.apradiso.2021.109776
Received 24 November 2020; Received in revised form 2 April 2021; Accepted 7 May 2021
Available online 13 May 2021

additional bystander signaling parameters to incorporate the bystander effects and dose gradients of the non-uniform Grid radiation field into the conventional LQ model. They showed that their extended model can accurately calculate the SF of cells after the MLC-based Grid irradiation, while the LQ model overestimated it.

In this study, we have applied both LQ and extended models to calculate TR and GSF of different Grid blocks and various delivered doses for breast cancer. Then, the results of the two models were compared to test the impact of radiobiological models on the calculation of TR, GSF, and SF of cancer and normal cells. Finally, the impact of the radiation dose and geometrical parameters on the differences between the two models' predictions were investigated. This evaluation was performed using the Monte Carlo simulation.

## 2. Materials and methods

### 2.1. Monte Carlo simulation

The Geant4 Monte Carlo code (Version 10.5), was employed to simulate dose distribution of 6 MV beam from Varian 2100/CD LINAC for Grid blocks with 20 geometrical designs in a $50 \times 50 \times 50$ cm$^3$ water phantom. The center of the phantom was positioned along the central axis of the beam. The distance between the upper surface of the phantom and the lower surface of the block tray was 34.6 cm. The accelerator head including target, primary collimator, beryllium window, flattening filter, and monitor unit ion chamber besides secondary collimator, was simulated.

The primary electron beam is defined as having a Gaussian energy and spatial distribution. For the spatial and energy distribution, FWHM was set equal to 2 mm and 3% of the mean energy (6 MeV), respectively. So, the standard deviation ($\sigma$) was 0.84932 and 0.01274 for the Gaussian spatial and energy distribution, respectively. These parameters were determined by trial and error, by performing comparisons between measured and simulated dose distributions (Oliveira et al., 2013).

A total number of $2 \times 10^9$ events were generated from the initial electron source. The variance reduction technique of bremsstrahlung splitting was used to create more than one secondary at an interaction. The range cut off was set at 1 mm; hence, the energy cut off in water was 5 keV for photons and 350 keV for electrons and positrons. Simple geometry biasing was implemented to save computing time. A killer cylinder was created around the head of the accelerator and the target to destroy particles unlikely to contribute to the dose distribution.

Cross-section libraries from the G4EmStandardPhysics_option4 physics list were employ to produce cross-section data for the photon and electron interactions (Arce et al., 2021).

A one-dimensional gamma index analysis (Low et al., 1998) was employed to verify the accuracy of the simulation, quantitatively. The water phantom was divided into a set of voxels with dimensions of $2 \times 2 \times 2$ mm$^3$ to calculate percentage depth dose (PDD) and dose profiles at a depth of 5 cm. The calculated PDD for $4 \times 4$, $10 \times 10$ and $20 \times 20$ cm open fields and beam profile at the depth of 5,10,15 cm for a $10 \times 10$ cm open field were compared with the experimental data obtained with the same field geometry and analyzed using a Gamma criterion of 2%-2 mm. The measurements were performed in Scanditronix blue phantom (Wellhofer. Germany) using a calibrated 0.13 cc ionization chamber.

### 2.2. Grid design

The structure of the Grid has been described in detail in the literature (Meigooni et al., 2006; Zhang et al., 2006). In brief, the blocks used in this study consist of a hexagonal pattern of divergent circular holes in 7 cm thick lead blocks located on the block tray position in Linac. The axes of the holes were also divergent to match the beam angle.

In total, 20 patterns of Grid block with different aperture sizes and center-to-center spacing were simulated to determine the optimal Grid design and to evaluate the impact of the Grid geometry on the differences between the two models. The diameters of holes were 0.5, 0.75, 1.0, 1.25, and 1.5 cm when projected to isocenter, and for each hole size, there were four center-to-center spacing (1.5, 1.7, 1.8, 2.0 cm).

We also calculated the valley to peak dose ratio (VPDR) and open to blocked area ratio (OBAR) as geometrical parameters of the Grid blocks. These geometrical parameters were then considered for the assessment of Grid block with different designs. The VPDR was calculated as the ratio of dose in the closed to the open regions in the profile dose distribution (at the depth of 5 cm), and OBAR were calculated from 2D projections of the Grid patterns at the isocenter. OBAR may depend on the field size, but in this study, the dosimetric data were all based on a constant Grid field size (10 cm × 10 cm) to ease of comparisons between different Grid blocks geometries.

### 2.3. Therapeutic ratio calculation

To evaluate the therapeutic advantage of Grid therapy, the methodology of Zwicker et al. (2004) has been used. The tissue volume under the central Grid hole was divided into the circular rings with 0.1 mm thickness, and it was assumed that all cells in each ring receive nearly the same radiation dose. We also assumed that the dose distribution of the holes is the same throughout the field. Therefore, only the dose distribution under the central hole was considered to compare different geometries. The maximum radius of rings was the same as the half of the hole spacing. Another assumption was that the normal cells were uniformly interspersed in the tumor volume. Therefore, the same dose distribution was used to calculate the SFs for tumoral and normal tissues. Under these assumptions, the average SF for tumoral and normal tissues in the Grid field was obtained by volume-weighted SF of individual rings using the LQ model:

$$\overline{SF}(Grid) = \sum V_i e^{\left(-\alpha.D_i-\beta.D_i^2\right)} \quad (1)$$

Where, $D_i$ and $V_i$ are the dose and volume percentage of each ring, respectively. In this study, we calculated the therapeutic parameters for breast cancer cell line (HCC-1945) and interspersed normal human umbilical vein endothelial cell line (HUVEC). The α and β for normal tissue were taken to be 0.249 Gy$^{-1}$ and 0.002 Gy$^{-2}$, respectively. For cancer cells, we used α = 0.320 Gy$^{-1}$ and β = 0.009 Gy$^{-2}$ (Peng et al., 2017).

To evaluate the impact of the bystander effect and dose gradient on the therapeutic parameters, an extended model was used to recalculate SF of normal and cancer tissues. The extended form of the LQ model for the calculation of SF was proposed by Peng (Peng et al., 2017) as follows:

$$\overline{SF}(Grid) = \sum V_i e^{\left[\left(-\alpha A.\overline{\mathbf{D}}\right)\mathbf{D_i}-\beta.\mathbf{D_i^2}\right]} \quad (2)$$

Where A is the bystander parameter which is directly related to the ability of cells to release bystander signaling factors, the ability of these factors to diffuse, and the ability of cells receiving the signals to respond, and $\overline{\mathbf{D}} = < \left|\frac{\partial \mathbf{D}}{\partial \mathbf{r}}\right| >$ is the average dose gradient, which determines the extent of diffusion of bystander signaling factors generated by the local dose ($D_i$). The bystander term is equal to the product of the bystander parameter (A), the local dose, and the average dose gradient. The values of bystander parameters for tumor and normal cells were considered to be 0.013 cm.Gy$^{-2}$ and 0.002 cm.Gy$^{-2}$, respectively. More detail about this model can be found elsewhere (Peng et al., 2017, 2018).

The average SF for the tumoral or normal cells in Grid therapy has the equivalent uniform dose (EUD), which is the equivalent single dose in a uniform radiation field that would results in the same SF for the cells across the tumoral or normal volume:

$$\overline{SF}(Grid) = e^{\left(-\alpha.EUD-\beta.EUD^2\right)} \quad (3)$$

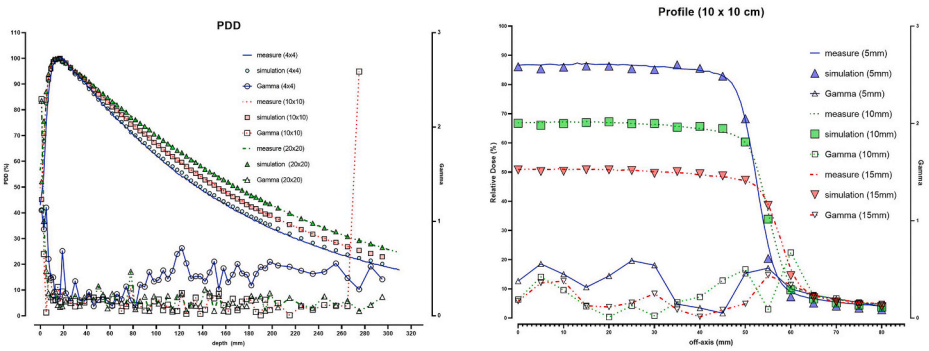


**Fig. 1.** A comparison between the simulated and measured PDD for 4×4, 10×10 and 20×20 cm open fields **(a)** and dose profile at the depth of 5,10,15 cm for a 10 × 10 cm open field **(b)** (with gamma criteria of 2%/2 mm).

Using equation (3), EUD was calculated for normal ($EUD_n$) and tumoral ($EUD_t$) cells. Finally, TRs and GSFs were calculated using equations (4) and (5), similar to that described in the literature (Zwicker et al., 2004; Gholami et al., 2017):

$$TR = \frac{\overline{SF}_n(\text{Grid})}{SF_n(EUD_t)} \tag{4}$$

$$GSF = \frac{EUD_n}{EUD_t} \tag{5}$$

$SF_n$ indicates the normal cell survival fraction. The TR parameter represents the degree of normal tissue protection, while the GSF parameter indicates the risk of normal tissue complications. In other words, a value of TR greater than 1 represents an increase in survival of normal tissue under Grid irradiation relative to those treated with an open field, while the tumor cell killing rate is the same in both cases. For a TR greater than 1, the lower value of the GSF shows the higher TR advantage.

A Grid block with hole diameter of 1.5 cm and hole spacing of 2 cm based on a commercially available GRID block (.decimal Inc., Sanford, FL) was considered in the comparison of the TR and GSF values for different Grid designs, and $EUD_t$ was calculated for this reference Grid block. For all other grid designs, the maximum prescription doses were adjusted so as to keep the $EUD_t$ at a constant value. In this condition, the SF for tumor cells with and without Grid is the same in all geometries. On the other hand, a constant $EUD_t$ leads to identical normal cell survival in the open field for all geometries. Therefore, changing the geometry will change only the $EUD_n$ and SF of normal cells in the Grid field. It should be noted that to compare the results of two models in the calculation of the $SF_t$ and $SF_n$, $EUD_t$ was variable among various Grid geometries.

### 2.4. Statistical analysis

The two independent samples *t*-test was employed using SPSS software (version 26.0) to assess the significance of the difference between two models in calculating TR and GSF. To this end, for a given hole diameter and dose, the average values of TR and GSF were calculated from the blocks with different center-to-center distances. Similarly, for a given hole spacing and dose, the average value of TR and GSF was calculated from the values for the blocks with different hole sizes. We also defined the relative difference between two model prediction as follow:

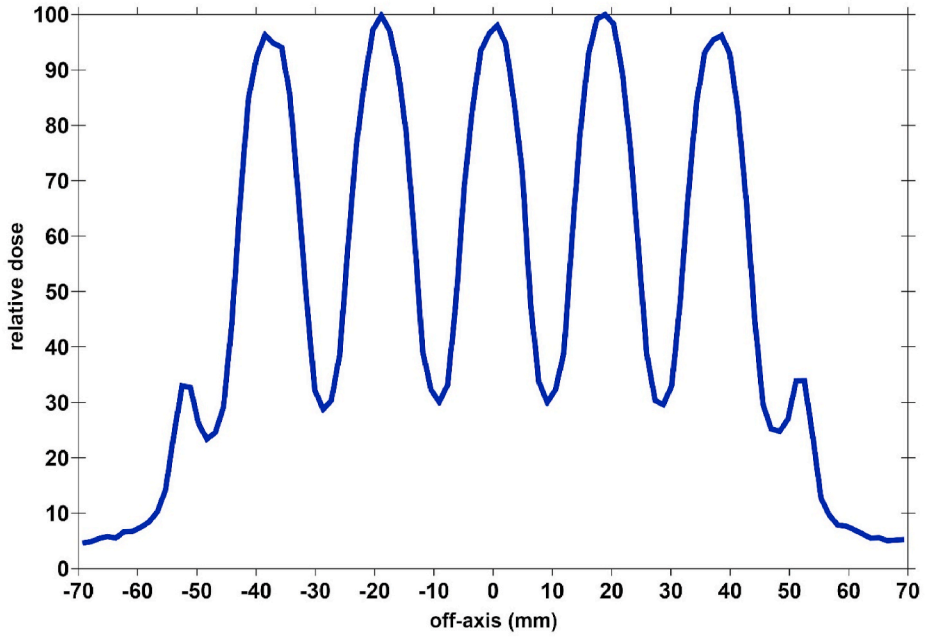


**Fig. 2.** The Monte Carlo simulated beam profile of a 6 MV spatially fractionated photon beam at 5 cm depth in water for a Grid block with 1.3 cm hole diameter and center-to-center spacing of 1.8 cm.

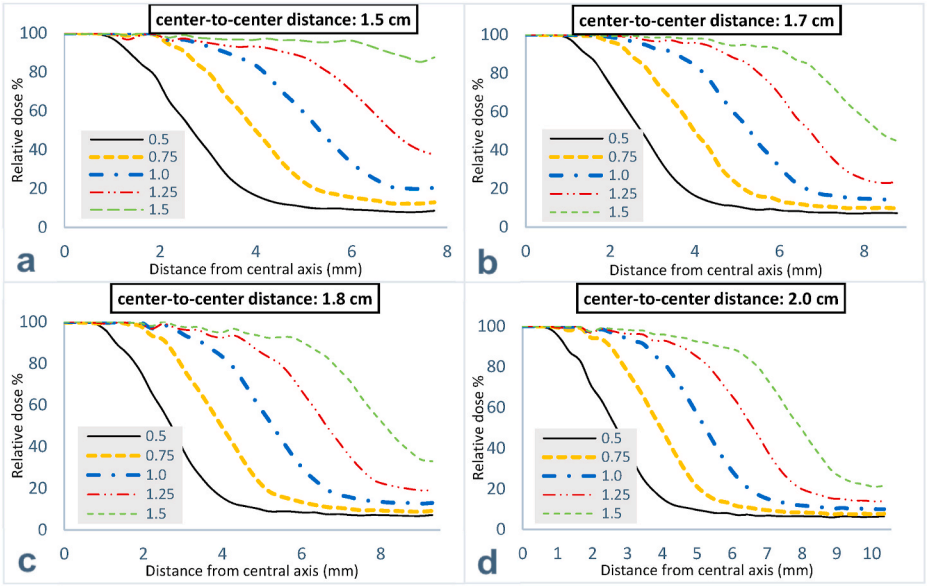


**Fig. 3.** Monte Carlo simulated dose semi-profiles of the Grid blocks with different hole diameters for (a) 1.5, (b) 1.7, (c) 1.8 and (d) 2.0 cm center-to-center distance.

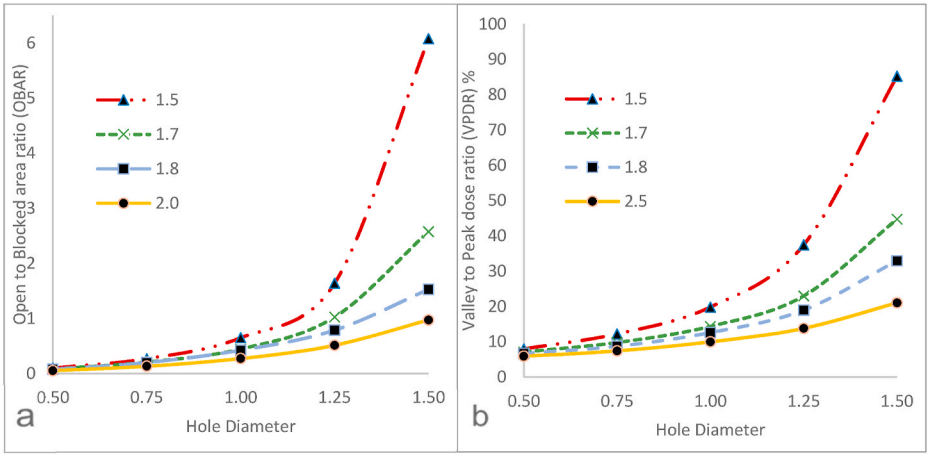


**Fig. 4.** Valley to peak dose ratio (a) and open to block area ratio (b) for different Grid blocks with different hole spacing as the function of hole diameter.

$$Relative\ difference(\%) = \frac{x_{LQ\ model} - x_{extended\ model}}{x_{LQ\ model}} \times 100 \quad (6)$$

Where "x" can be defined as SF, GSF or TR. Pearson's correlation coefficient was used to determine the relation between geometrical parameters and relative differences of two models in calculating therapeutic parameter. Statistically, a significant difference was defined at a level of P-value $< 0.05$. Furthermore, maximum doses of 5,10, 15, 20, and 25 Gy were used to investigate the role of the prescription dose on the relative differences between the two models' predictions. Maximum doses were prescribed at a depth of 5 cm.

## 3. Results

### 3.1. Monte Carlo simulation

The MC-simulated PDD and beam profile for open fields show good agreement with measurements, by a passing rate of over 97% for the points with a 2%-2 mm gamma criterion (Fig. 1). The statistical uncertainties of the Monte Carlo simulation were less than 1%.

A Monte Carlo simulated 2D profile at the depth of 5 cm in water in the presence of a Grid with 1.3 cm hole diameter and 1.8 center-to-center distances was shown in Fig. 2.

Fig. 3 shows half of the MC simulated dose profiles at 5-cm depth for Grid blocks with hole diameters of 0.5, 0.75, 1.0, 1.25, and 1.5 cm, with a grid spacing of 1.5, 1.7, 1.8, and 2.0 cm.

### 3.2. Geometric and therapeutic parameters calculations

Fig. 4 represents the valley to peak dose ratio (VPDR) and open to block area ratio (OBAR) as the functions of hole diameter and hole spacing. It was found that the VPDR and OBAR significantly increase with the hole diameter and decrease with hole spacing.

To compare the TRs and GSFs of various block designs, maintaining the clinical effectiveness of the reference Grid block (with a hole diameter of 1.5 cm and hole spacing of 2.0 cm) on tumor cells was desired. For this purpose, as the block geometries varied, the maximum prescription dose was also varied so as to keep the EUD and SF of cancer cells at a constant value. The table below shows the variation of the prescription dose (15 Gy is depicted here, as an example) for various Grid designs for both standard and extended LQ models.

Both the block geometry and maximum dose can affect the average dose gradient. As shown in Table 1, changing the hole diameter and hole spacing of the Grid block also significantly changed the maximum dose.

**Table 1**
Equivalent 15 Gy dose in the Grid block with a hole diameter of 1.5 cm and hole spacing of 2.0 cm for various block designs.

| | | Equivalent 15 Gy dose (Gy) | | | | | | | | | | | |
|---|---|---|---|---|---|---|---|---|---|---|---|---|---|
| | | center-to-center distance (cm) | | | | | | | | | | | |
| | | 1.5 | | | 1.7 | | | 1.8 | | | 2.0 | | |
| | | LQ model | extended model | Relative Differences% | LQ model | extended model | Relative Differences% | LQ model | extended model | Relative Differences% | LQ model | extended model | Relative Differences% |
| hole size (cm) | **0.5** | 56.7 | 49.1 | **13.4** | 65.6 | 56.5 | **13.9** | 71.1 | 61.0 | **14.2** | 81.3 | 69.4 | **14.6** |
| | **0.75** | 33.5 | 30.9 | **7.8** | 44.6 | 40.5 | **9.2** | 50.0 | 45.0 | **10.0** | 61.1 | 54.1 | **11.5** |
| | **1.0** | 18.2 | 17.8 | **2.2** | 27.3 | 26.1 | **4.4** | 31.9 | 30.1 | **5.6** | 42.5 | 39.3 | **7.5** |
| | **1.25** | 9.3 | 9.4 | **−1.1** | 14.5 | 14.4 | **0.7** | 18.1 | 17.8 | **1.7** | 26.9 | 26.0 | **3.3** |
| | **1.5** | 6.4 | 6.5 | **−1.6** | 8.1 | 8.2 | **−1.2** | 9.7 | 9.8 | **−1.0** | 15 | 15 | **0.0** |

For a given hole spacing and dose, the average dose gradient decreased with hole diameter, and for a given hole diameter and dose, the average dose gradient increased with hole spacing, if a constant EUD was considered for all blocks (see Fig. 5). However, when varying EUD was used for individual blocks, the average dose gradient decreased with hole diameter and hole separation. Furthermore, a significant positive correlation was found between the average dose gradient and prescription dose, whether EUD was constant or not.

The standard LQ model over-predicts SF of both cancer and normal cell lines for all Grid designs, especially at higher doses. The largest difference between the two models in the prediction of SFs was found at the dose of 25 Gy and for the Grid block with the hole diameter of 1.25 cm and hole spacing of 1.5 cm (26.81% and 5.16% for cancer and normal cell lines, respectively). The minimum difference between the two models in the calculation of SFs was obtained at the dose of 5 Gy and for a Grid block with the hole diameter of 0.5 cm and hole spacing of 2.0 cm (0.3% and 0.05% for cancer and normal cell lines, respectively). Furthermore, a statistically significant increase was seen in the relative difference between the two models for cancer and normal SF calculation when the VPDR and OBAR values were increased.

We also made a comparison between standard and extended LQ models for predicting TR and GSF for the different block designs and various prescription doses. As shown in Table 2, a Grid with hole size and hole spacing of 1.5 cm had the lowest average dose gradient and maximum VPDR and OBAR. According to the LQ predictions, irradiation using this Grid block would lead to the maximum TR and minimum GSF. However, based on the results of the extended model, the maximal TR and minimal GSF were obtained by a Grid with the hole size of 0.5 cm and the hole spacing of 2.0 cm (largest average dose gradient and minimal VPDR and OBAR)

Compared to the LQ model, at all prescription doses and block designs, the extended model predicts a higher value for the TR and a lower value for the GSF.

For a prescription dose of 15 Gy, a significant difference in the TR and GSF values is found between two models at lower hole sizes (0.5, 0.75, and 1.0 cm). However, the significance is lost for the larger hole sizes (1.25 and 1.5 cm). If higher prescription doses were used, the difference between the TR and GSF values from both models was statistically significant even for large hole sizes. A statistically significant difference was not observed between the two models for the lower prescription doses, even for lower hole diameters. In was found that the relative differences between two models in the calculation of TR and GSF values significantly increase with an increase in the hole spacing and prescription and decrease in the hole size and VPDR.

The difference between the two models in calculating the TR and GSF values is maximal (42.44% and 14.15%, respectively) for the Grid block with a hole diameter of 0.5 cm and a hole spacing of 2.0 cm, and prescription dose of 25 Gy. The lowest differences between TR and GSF values from both standard and extended LQ models (0.19% and 0.097%, respectively) were obtained for the Grid block with hole diameter and hole spacing of 1.5 cm and a prescription dose of 5 Gy. These results indicate that the relative differences between the two models in the calculation of TR and GSF values are dependent on the average dose gradient so that the relative differences between the two models significantly increase with the average dose gradient. In low average dose gradient, the calculated TR and GSF using the LQ model are nearly the same as that of the extended model, while the results for the higher average dose gradient are significantly different.

## 4. Discussion

Prior studies have noted the importance of the bystander effects in the cellular response to highly modulated radiation fields such as used in Grid therapy (Asur et al., 2012, 2015; Peng et al., 2017, 2018). The conventional LQ models, however, do not incorporate these effects in the calculations. In the present study, we have used an extended

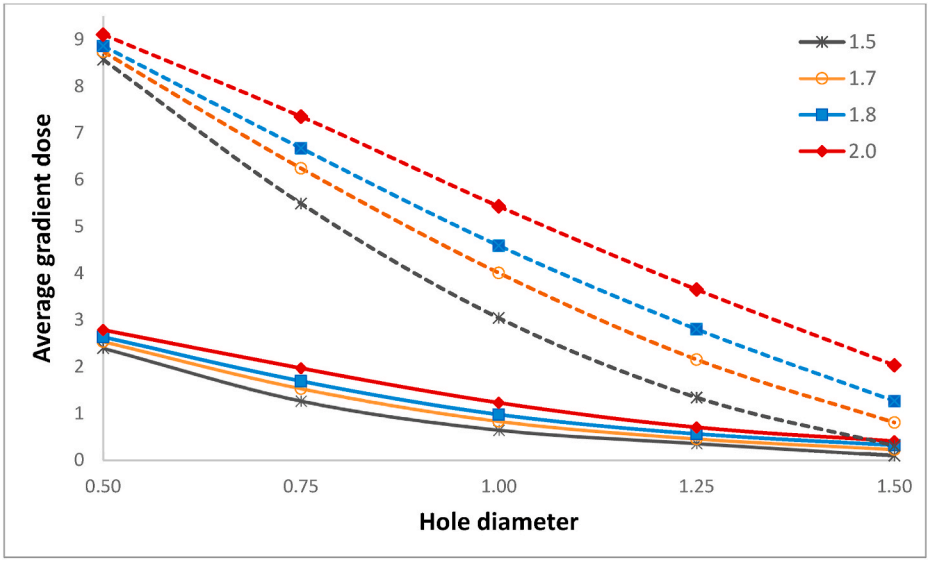


**Fig. 5.** The average dose gradient of Grid blocks with different hole sizes and hole spacing for the prescription dose of 25 Gy (dashed) and 5 Gy (solid). (The prescription doses of 25 Gy and 5 Gy were displayed for simplicity. Other doses also show a similar trend).

radiobiological model—introduced by Peng et al. (2017)—to incorporate the bystander effects into the calculation of cell survival in Grid radiation fields. In this investigation, we have provided a dosimetric simulation of 20 Grid blocks with different geometries and various doses for assessing the relative differences between the standard and extended LQ models in the calculation of therapeutic parameters of Grid therapy.

Our results show that the predicted SFs for both cancer and normal cell lines using the extended model are lower than those predicted from the standard LQ model, especially at higher doses. This results in an increase in the EUD for the extended LQ model compared with the standard LQ model. This finding is in agreement with Butterworth's reports, which showed that incorporating the bystander effects in the calculations reducing the SF and increasing EUD for GRID exposures compared with standard models (Butterworth et al., 2017). This also accords with Peng (Peng et al., 2017) observations, which indicated that the prediction of the extended model is not significantly different from the experimental survival for cancer cell lines, while the standard LQ model gives rise to the significant deviations from the experimental values. This study also supports evidence from experimental data showing that the out-of-field survival of both cancer and normal cell lines following non-uniform exposure is dramatically less than predicted from the standard LQ model (Butterworth et al., 2011, 2012). This discrepancy could be attributed to the cytotoxic bystander effect, which appears as the "A parameter" in the extended LQ model.

As discussed, the local dose is responsible for generating the bystander signals, and the average dose gradient determines the extent of their distribution. Both generated signals and the average dose gradient is increased as the maximum dose increases. In these conditions, more biological effects are induced, and the overall survival is more influenced. So, the discrepancy between the two models would be more significant at higher doses. An experimental demonstration of this effect was carried out by Butterworth et al. (2012). They created a non-uniform radiation field by shielding a portion of the field from the primary beam and showed that the survival of the shielded cells for both cancer and normal cell lines reduced with an increase in the dose delivered to the un-shielded region. This reduction in the shielded cell survival was shown to be significantly more than that predicted solely based on scattered dose and was attributed to the bystander effects.

In addition, the results indicate that the relative differences between the two models in the calculation of SF of normal cells are less than that for cancer cells. This may be explained by the fact that the HUVEC normal cell line has a smaller value of "A parameter" than for the HCC-1954 breast cell lines. This suggests that either the cytotoxic effect of bystander signaling is less in the normal cell line or there are additional components of the bystander effect, which encouraging cell proliferation.

It was found that the average dose gradient is sensitive to both the Grid design and maximum dose. The dose gradient generated from spatial modulation results in the deviation of the LQ model predictions from that of the extended model. For low average dose gradient, for example, a Grid with hole size and hole spacing in the order of 1.5 cm and maximum dose of 5 Gy, calculating the TR and the GSF using the standard LQ model may be acceptable and would not change the conclusions of Grid therapy. However, when the average dose gradient is high, for example, a prescription dose of 25 Gy along with a Grid with a hole size of 0.5 cm and a hole spacing of 2.0 cm, the results from two models would significantly be different (P-value$<$0.05). These results are in agreement with experimental data from Peng et al. (2017). Therefore, it is not recommended that the standard LQ model be used to predict Grid therapy outcomes in fields containing high dose gradients. This is an important issue that suggests that the bystander effect must be included in the TR and GSF calculations for future research.

The calculated TR and GSF values using the LQ model indicate that a Grid with hole size and hole spacing of 1.5 cm have optimal therapeutic parameters (maximum TR and minimum GSF). This block design has the lowest average dose gradient and maximum VPDR and OBAR. What is surprising is that the extended model suggests a Grid block with the hole size of 0.5 cm and the hole spacing of 2.0 cm as the optimal Grid block. In contrast to that recommended by the LQ model, this block has the largest average dose gradient and minimal VPDR and OBAR. These results challenge the previous works that used the standard LQ model to introduce recommendations for selecting the optimal Grid design (Gholami et al., 2016, 2017; Sathishkumar et al., 2002; Costlow et al., 2014; Zhang et al., 2008).

The current data highlight the importance of bystander effects in evaluating Grid efficiency. However, a limitation of this study is that it has examined the Grid efficacy for only one type of tumor and normal cells. The results may be different for other cell lines with different radiosensitivity. Therefore, further investigations are required to validate these effects in vivo and develop a reliable theoretical method for assessing the clinical benefits of Grid therapy.

**Table 2**
TR and GSF values for different Grid blocks with different hole sizes and hole spacing for the prescription dose of 15 Gy.

| | | TR | | | | | | | | | | | |
|---|---|---|---|---|---|---|---|---|---|---|---|---|---|
| | | center-to-center-distance (cm) | | | | | | | | | | | |
| | | 1.5 | | | 1.7 | | | 1.8 | | | 2.0 | | |
| | | LQ model | extended model | Relative Difference% | LQ model | extended model | Relative Difference% | LQ model | extended model | Relative Difference% | LQ model | extended model | Relative Difference% |
| hole size (cm) | **0.5** | 0.90 | 1.08 | **−19.73** | 0.91 | 1.10 | **−20.53** | 0.92 | 1.12 | **−21.14** | 0.93 | 1.14 | **−22.05** |
| | **0.75** | 0.85 | 0.95 | **−11.45** | 0.87 | 0.99 | **−13.56** | 0.88 | 1.01 | **−14.75** | 0.89 | 1.04 | **−16.69** |
| | **1.0** | 0.83 | 0.87 | **−5.49** | 0.83 | 0.89 | **−7.73** | 0.84 | 0.91 | **−9.13** | 0.85 | 0.95 | **−11.35** |
| | **1.25** | 0.93 | 0.96 | **−2.67** | 0.83 | 0.86 | **−3.42** | 0.81 | 0.85 | **−4.71** | 0.81 | 0.86 | **−6.64** |
| | **1.5** | 1.00 | 1.01 | **−0.83** | 0.96 | 0.97 | **−1.65** | 0.91 | 0.93 | **−2.16** | 0.82 | 0.84 | **−2.91** |
| GSF | | | | | | | | | | | | | |
| hole size (cm) | **0.5** | 1.06 | 0.95 | **10.28** | 1.06 | 0.94 | **10.73** | 1.05 | 0.93 | **11.07** | 1.04 | 0.92 | **11.56** |
| | **0.75** | 1.10 | 1.03 | **6.12** | 1.08 | 1.01 | **7.19** | 1.08 | 0.99 | **7.80** | 1.07 | 0.98 | **8.79** |
| | **1.0** | 1.11 | 1.08 | **3.11** | 1.12 | 1.07 | **4.23** | 1.11 | 1.05 | **4.94** | 1.10 | 1.03 | **6.06** |
| | **1.25** | 1.04 | 1.03 | **1.62** | 1.11 | 1.09 | **2.06** | 1.13 | 1.10 | **2.72** | 1.13 | 1.09 | **3.68** |
| | **1.5** | 1.00 | 1.00 | **0.49** | 1.03 | 1.02 | **1.02** | 1.06 | 1.04 | **1.35** | 1.12 | 1.10 | **1.80** |

## 5. Conclusion

This study set out to investigate the impact of the bystander effects on the calculation of therapeutic parameters of Grid therapy. In this investigation, we have examined the differences between the standard LQ model and the extended LQ model with an additional bystander signaling term describing the cell signaling effects.

The results indicate that incorporating bystander effects within the radiobiological models have a significant impact on the calculation of the therapeutic parameters of Grid therapy for breast cancer. The standard LQ model over-predicts the survival for both cancer and normal cell lines, especially at higher doses. In addition, it predicts a lower value for the TR and a higher value for the GSF at all prescription doses and block designs, in compare to the extended model. The research also shows that the discrepancy between the two models significantly increases with the dose gradient. Therefore, it is not recommended that the standard LQ model be used to predict Grid therapy outcomes, especially in fields containing high dose gradients.

## Funding

This study is a part of MSc thesis of Farshid Mahmoodi which was financially supported by Jundishapur University of Medical Sciences (Grant No. U-95128)

## Compliance with ethical standards

This article does not contain any studies with human participants or animals performed by any of the authors.

## CRediT authorship contribution statement

**Farshid Mahmoudi:** Conceptualization, Methodology, Writing – original draft, Software, Investigation. **Nahid Chegeni:** Conceptualization, Methodology, Supervision, Data curation, Writing – review & editing, Funding acquisition. **Ali Bagheri:** Conceptualization, Methodology, Validation. **Jafar Fatahi Asl:** Formal analysis, Resources. **Mohammad Taghi Batiar:** Software, Validation.

## Declaration of competing interest

The authors declare that they have no known competing financial interests or personal relationships that could have appeared to influence the work reported in this paper.

## References

Arce, P., Bolst, D., Bordage, M.C., Brown, J., Cirrone, P., Cortés-Giraldo, M., et al., 2021. Report on G4-Med, a Geant4 benchmarking system for medical physics applications developed by the Geant4 Medical simulation benchmarking group. Med. Phys. 48, 19–56.

Asur, R.S., Sharma, S., Chang, C.-W., Penagaricano, J., Kommuru, I.M., Moros, E.G., et al., 2012. Spatially fractionated radiation induces cytotoxicity and changes in gene expression in bystander and radiation adjacent murine carcinoma cells. Radiat. Res. 177, 751–765.

Asur, R., Butterworth, K.T., Penagaricano, J.A., Prise, K.M., Griffin, R.J., 2015. High dose bystander effects in spatially fractionated radiation therapy. Canc. Lett. 356, 52–57.

Bromley, R., Oliver, L., Davey, R., Harvie, R., Baldock, C., 2008. Predicting the clonogenic survival of A549 cells after modulated x-ray irradiation using the linear quadratic model. Phys. Med. Biol. 54, 187.

Butterworth, K.T., McGarry, C.K., Trainor, C., O'Sullivan, J.M., Hounsell, A.R., Prise, K. M., 2011. Out-of-field cell survival following exposure to intensity-modulated radiation fields. Int. J. Radiat. Oncol. Biol. Phys. 79, 1516–1522.

Butterworth, K.T., McGarry, C.K., Trainor, C., McMahon, S.J., O'Sullivan, J.M., Schettino, G., et al., 2012. Dose, dose-rate and field size effects on cell survival following exposure to non-uniform radiation fields. Phys. Med. Biol. 57, 3197.

Butterworth, K.T., Ghita, M., McMahon, S.J., Mcgarry, C.K., Griffin, R.J., Hounsell, A.R., et al., 2017. Modelling responses to spatially fractionated radiation fields using preclinical image-guided radiotherapy. Br. J. Radiol. 90, 20160485.

Choi, J.I., Daniels, J., Cohen, D., Li, Y., Ha, C.S., Eng, T.Y., 2019. Clinical outcomes of spatially fractionated GRID radiotherapy in the treatment of bulky tumors of the head and neck. Cureus 11.

Costlow, H.N., Zhang, H., Das, I.J., 2014. A treatment planning approach to spatially fractionated megavoltage grid therapy for bulky lung cancer. Med. Dosim. 39, 218–226.
Dubben, H.-H., Thames, H.D., Beck-Bornholdt, H.-P., 1998. Tumor volume: a basic and specific response predictor in radiotherapy. Radiother. Oncol. 47, 167–174.
Gholami, S., Nedaie, H.A., Longo, F., Ay, M.R., Wright, S., Meigooni, A.S., 2016. Is grid therapy useful for all tumors and every grid block design? J. Appl. Clin. Med. Phys. 17.
Gholami, S., Nedaie, H.A., Longo, F., Ay, M.R., Dini, S.A., Meigooni, A.S., 2017. Grid block design based on monte carlo simulated dosimetry, the linear quadratic and Hug–Kellerer radiobiological models. J. Med. Phys. 42, 213.
Huhn, J.L., Regine, W.F., Valentino, J.P., Meigooni, A.S., Kudrimoti, M., Mohiuddin, M., 2006. Spatially fractionated GRID radiation treatment of advanced neck disease associated with head and neck cancer. Technol. Canc. Res. Treat. 5, 607–612.
Kaiser, A., Mohiuddin, M.M., Jackson, G.L., 2013. Dramatic response from neoadjuvant, spatially fractionated GRID radiotherapy (SFGRT) for large, high-grade extremity sarcoma. Journal of Radiation Oncology 2, 103–106.
Low, D.A., Harms, W.B., Mutic, S., Purdy, J.A., 1998. A technique for the quantitative evaluation of dose distributions. Med. Phys. 25, 656–661.
McMahon, S.J., McGarry, C.K., Butterworth, K.T., Jain, S., O'Sullivan, J.M., Hounsell, A. R., et al., 2015. Cellular signalling effects in high precision radiotherapy. Phys. Med. Biol. 60, 4551.
Meigooni, A., Malik, U., Zhang, H., Dini, S., Meigooni, N., Komanduri, K., et al., 2005. Grid: a location dependent intensity modulated radiotherapy for bulky tumors. Iranian Journal of Radiation Research (Print) 2, 167–174.
Meigooni, A.S., Dou, K., Meigooni, N.J., Gnaster, M., Awan, S., Dini, S., et al., 2006. Dosimetric characteristics of a newly designed grid block for megavoltage photon radiation and its therapeutic advantage using a linear quadratic model. Med. Phys. 33, 3165–3173.
Mohiuddin, M., Stevens, J.H., Reiff, J.E., Huq, M.S., Suntharalingam, N., 1996. Spatially fractionated (GRID) radiation for palliative treatment of advanced cancer. Radiat. Oncol. Invest. 4, 41–47.
Mohiuddin, M., Fujita, M., Regine, W.F., Megooni, A.S., Ibbott, G.S., Ahmed, M.M., 1999. High-dose spatially-fractionated radiation (GRID): a new paradigm in the management of advanced cancers. Int. J. Radiat. Oncol. Biol. Phys. 45, 721–727.
Oliveira, A.C., Santana, M.G., Lima, F.R., Vieira, J.W., 2013. Monte Carlo Simulation of a Medical Linear Accelerator for Generation of Phase Spaces.
Penagaricano, J.A., Griffin, R., Corry, P., Moros, E., Yan, Y., Ratanatharathorn, V., 2009. Spatially fractionated (GRID) therapy for large and bulky tumors. J. Ark. Med. Soc. 105, 263–265.
Peng, V., Suchowerska, N., Rogers, L., Claridge Mackonis, E., Oakes, S., McKenzie, D.R., 2017. Grid therapy using high definition multileaf collimators: realizing benefits of the bystander effect. Acta Oncol. 56, 1048–1059.
Peng, V., Suchowerska, N., Esteves, A.D.S., Rogers, L., Mackonis, E.C., Toohey, J., et al., 2018. Models for the bystander effect in gradient radiation fields: range and signalling type. J. Theor. Biol. 455, 16–25.
Sathishkumar, S., Dey, S., Meigooni, A.S., Regine, W.F., Kudrimoti, M., Ahmed, M.M., et al., 2002. The impact of TNF-α induction on therapeutic efficacy following high dose spatially fractionated (GRID) radiation. Technol. Canc. Res. Treat. 1, 141–147.
Suchowerska, N., Ebert, M.A., Zhang, M., Jackson, M., 2005. In vitro response of tumour cells to non-uniform irradiation. Phys. Med. Biol. 50, 3041.
Zhang, H., Johnson, E.L., Zwicker, R.D., 2006. Dosimetric validation of the MCNPX Monte Carlo simulation for radiobiologic studies of megavoltage grid radiotherapy. Int. J. Radiat. Oncol. Biol. Phys. 66, 1576–1583.
Zhang, H., Wang, J.Z., Mayr, N., Kong, X., Yuan, J., Gupta, N., et al., 2008. Fractionated grid therapy in treating cervical cancers: conventional fractionation or hypofractionation? Int. J. Radiat. Oncol. Biol. Phys. 70, 280–288.
Zhang, H., Zhong, H., Barth, R.F., Cao, M., Das, I.J., 2014. Impact of dose size in single fraction spatially fractionated (grid) radiotherapy for melanoma. Med. Phys. 41, 021727.
Zwicker, R.D., Meigooni, A., Mohiuddin, M., 2004. Therapeutic advantage of grid irradiation for large single fractions. Int. J. Radiat. Oncol. Biol. Phys. 58, 1309–1315.